The Cryosphere Discuss., doi:10.5194/tc-2016-64, 2016
Manuscript under review for journal The Cryosphere
Published: 13 April 2016

The Cryosphere Discussions
Open Access

Snow fracture in relation to slab avalanche release: critical state for the onset of crack propagation

Johan Gaume[1], Alec van Herwijnen[1], Guillaume Chambon[2,3], Nander Wever[1,4], and Jürg Schweizer[1]

[1]WSL Institute for Snow and Avalanche Research SLF, Davos, Switzerland
[2]Irstea, UR ETGR, Grenoble, France
[3]Université Grenoble Alpes, Grenoble, France
[4]École Polytechnique Fédérale de Lausanne (EPFL), Lausanne, Switzerland

Correspondence to: Johan Gaume (gaume@slf.ch)

Abstract. The failure of a weak snow layer buried below cohesive slab layers is a necessary, but insufficient condition for the release of a dry-snow slab avalanche. The size of the crack in the weak layer must also exceed a critical length to propagate over a wide surface. In contrast to pioneering shear-based approaches, recent developments account for weak layer collapse and ~~allow for better explaining~~ typical observations of remote triggering from flat areas. However, these new models predict a critical length for crack propagation that is almost independent of slope angle, a rather surprising and counterintuitive result. Our new mechanical model reconciles past approaches by considering for the first time the complex interplay between slab elasticity and the mechanical behaviour of the weak layer including its structural collapse. The crack begins to propagate when the stress induced by slab loading and deformation at the crack tip exceeds the limit given by the failure envelope of the weak layer. We are able to reproduce crack propagation on flat terrain and the decrease in critical length with slope angle modeled in numerical experiments. The good agreement of our new model with extensive field data and its successful implementation in the snow cover model SNOWPACK opens promising prospect towards improving avalanche forecasting.

1 Introduction

Snow slab avalanches ~~range~~ among the most prominent natural hazards in snow covered mountainous regions throughout the world. The winter 2014/2015 served as a cruel reminder of the destructive power of this ~~ubiquitous~~ natural hazard with 132 fatalities, just for the European Alps. The ability to reliably forecast avalanche danger is therefore of vital importance and requires a sound understanding of avalanche release processes.

The Cryosphere Discuss., doi:10.5194/tc-2016-64, 2016
Manuscript under review for journal The Cryosphere
Published: 13 April 2016

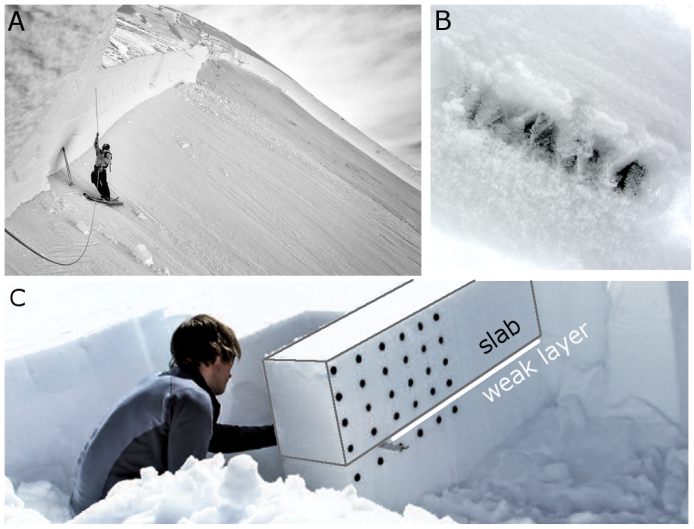

Figure 1: (a) Crown fracture of a dry-snow slab avalanche in Mt Baker, USA ©Grant Gunderson . (b) Surface hoar weak layer. (c) Propagation Saw Test. The weak layer is represented in white, the slab in grey. The black dots are markers used for particle tracking to measure slab deformation.

Avalanches are the result of numerous factors and processes interacting over a large range of temporal and spatial scales (Schweizer et al., 2003). While snow slab avalanches can come in many different sizes, from a few meters to several kilometers, they initiate within the snow cover by local damage processes at the grain scale. Indeed, the release of a dry-snow slab avalanche (Fig. 1a) requires the formation of a localized failure within a so-called weak layer (WL) buried below cohesive slab layers (Fig. 1b). The initial failure – or crack – in the WL either forms in weak parts of the snowpack (Schweizer et al., 2008; Gaume et al., 2014b), or below a local overload such as a skier or a snowmobile (van Herwijnen and Jamieson, 2005; Thumlert and Jamieson, 2014). Stress concentrations at the crack tip~~s~~ will then determine if crack propagation and eventually slope failure occurs (McClung, 1979; Schweizer et al., 2003), even if the average overlying stress is lower than the average weak layer strength (knock-down effect, Fyffe and Zaiser, 2004; Gaume et al., 2013, 2014b). The size of the initial crack at which rapid crack propagation occurs is called cri(cal) crack length and represents an instability criterion material failure (Anderson, 2005). It is a crucial variable to evaluate snow slope instability (Reuter et al., 2015).

Information on snow cover stratigraphy, especially the presence and characteristics of WLs and the overlying slab, is thus essential for avalanche forecasting. Traditionally, such information is obtained through manual snow cover observations, such as snow profiles and stability tests (Schweizer and Jamieson, 2010). However, these observations are time consuming, somewhat subjective and only provide point observations. Snow cover models such as CROCUS (Brun et al., 1992) or SNOW-

The Cryosphere Discuss., doi:10.5194/tc-2016-64, 2016
Manuscript under review for journal The Cryosphere
Published: 13 April 2016

PACK (Lehning et al., 1999) provide a valuable alternative to obtain more highly resolved snow stratigraphy data. However, to evaluate snow slope instability based on model output, avalanche formation processes are greatly simplified, and reduced to accounting for the balance between shear strength of the WL and shear stress due to the weight of the overlying slab, sometimes including a skier overload (Schweizer et al., 2006; Monti et al., 2016). This 'strength-over-stress' approach is only relevant for failure initiation and does not account for crack propagation, the second fundamental process in avalanche release.

Due to the very complex nature of crack propagation in multilayered elastic systems under mixed-mode loading, theoretical and analytical approaches are not yet conceivable (Hutchinson and Suo, 1992). In the past, simplifying assumptions have been used to propose analytical models for critical crack length. For instance, McClung (1979); Chiaia et al. (2008); Gaume et al. (2014b) assumed a weak layer without thickness which allowed to solve the problem in the down-slope direction only, by neglecting the effect of the volumetric collapse of the weak layer. On the other hand, Heierli et al. (2008) assumed a weak layer of finite thickness with a slope-independent failure criterion and a completely rigid behavior allowing to neglect the elastic mismatch between the slab and the weak layer. With the development of new field tests, in particular the propagation saw test (PST, Fig. 1c) (van Herwijnen and Jamieson, 2005; Gauthier and Jamieson, 2006; Sigrist and Schweizer, 2007), it is now possible to directly evaluate critical crack length, and thus determine crack propagation propensity. Particle tracking velocimetry (PTV) analysis of PSTs has highlighted the importance of the elastic bending of the slab induced by the loss of slab support due to weak layer failure prior to crack propagation (van Herwijnen and Heierli, 2010; van Herwijnen and Birkeland, 2014). To include this process in the description of slab avalanche release mechanisms, Heierli et al. (2008) proposed the anticrack model. This model provides an analytical framework to estimate critical crack length as a function of slab properties (thickness, density and elastic modulus) and the WL specific fracture energy, a WL property quantifying the resistance to crack propagation. While some crucial features of the mechanical behavior of the WL, including elasticity and shape of the failure envelope are not included, the anticrack model provides a significant step forward as it accounts for various aspects that were left unexplained by previous theories, such as crack propagation on flat terrain and remote triggering of avalanches.

To evaluate critical crack length based on the anticrack model, WL specific fracture energy is required. It can be estimated using three different methods: (i) through PTV or finite element analysis of the PST (Sigrist and Schweizer, 2007; van Herwijnen and Heierli, 2010; Schweizer et al., 2011); (ii) from snow micro-penetrometer (SMP) measurements (Schneebeli et al., 1999) by integrating the penetration resistance over the thickness of the WL (Reuter et al., 2015) and (iii) from X-ray computer tomography-based (CT) microstructural models (LeBaron and Miller, 2014). Depending on the method, estimates of the WL specific fracture energy can differ by as much as two orders of magnitude, resulting in widely different values of critical crack length. Strength-of-material approaches

The Cryosphere Discuss., doi:10.5194/tc-2016-64, 2016
Manuscript under review for journal The Cryosphere
Published: 13 April 2016

have also been developed to evaluate the conditions for the onset of crack propagation (Chiaia et al., 2008; Gaume et al., 2013, 2014b). These methods require WL strength, a property which is more readily measurable (Jamieson and Johnston, 2001), rather than the specific fracture energy. Yet, in contrast to the anticrack model, strength-of-material approaches do not account for slab bending which leads to additional stress concentrations, hence these models tend to overestimate the critical length.

Clearly, the various methods to estimate critical crack length all have their respective shortcomings, and a unified approach which incorporates all relevant processes is thus far missing. To overcome these limitations and take into account all the important physical ingredients, we propose to evaluate critical crack length for different snowpack stratigraphies using discrete element (DEM) simulations. Similar to the field experiments, in the simulations we gradually create a crack in the WL with a saw until rapid propagation occurs (Fig. 2). On the basis of our numerical results, we then introduce a new expression for critical crack length which accounts, for the first time, for the complex interplay between loading, elasticity, failure envelope of the WL and its structural collapse. The predictive capabilities of this new expression, with respect to field data, are discussed and compared to previous models.

2 Methods

Discrete element model

We model crack propagation in a slab-WL system using the discrete element method (DEM). DEM is well suited to represent large deformations as well as the evolution of the microstructure of materials in a dynamic context (Radjai et al., 2011; Hagenmuller et al., 2015; Gaume et al., 2015). The simulations are performed using PFC2D (by Itasca), implementing the original soft-contact algorithm of Cundall and Strack (1979). The numerical setup is fully described in Gaume et al. (2015). We recall here its main characteristics.

The simulated system (Fig. 2a) is 2D and composed of a fixed substratum, a WL of thickness D_{wl} (varied between 0.02 and 0.06 m) and a slab of thickness D (varied between 0.2 and 0.8 m). The slab is modeled with spherical elements of radius $r = 0.01$ m with a square packing. As explained in Gaume et al. (2015), these elements are not intended to represent the real snow grains. They constitute entities of discretization used to model an elastic continuum of density ρ, Young's modulus E and Poisson's ratio ν. The WL is composed of elements of radius $r_{wl} = r/2$ with a packing of collapsible triangular shapes of the same size as the WL thickness (Fig. 2a) aimed at roughly representing the porous microstructure of persistent WLs such as surface hoar (Fig. 1b) or depth hoar.

We used the cohesive contact law detailed in Gaume et al. (2015). The bonds are characterized by specific elasticity and strength parameters which have been calibrated to obtain the desired macro-

The Cryosphere Discuss., doi:10.5194/tc-2016-64, 2016
Manuscript under review for journal The Cryosphere
Published: 13 April 2016

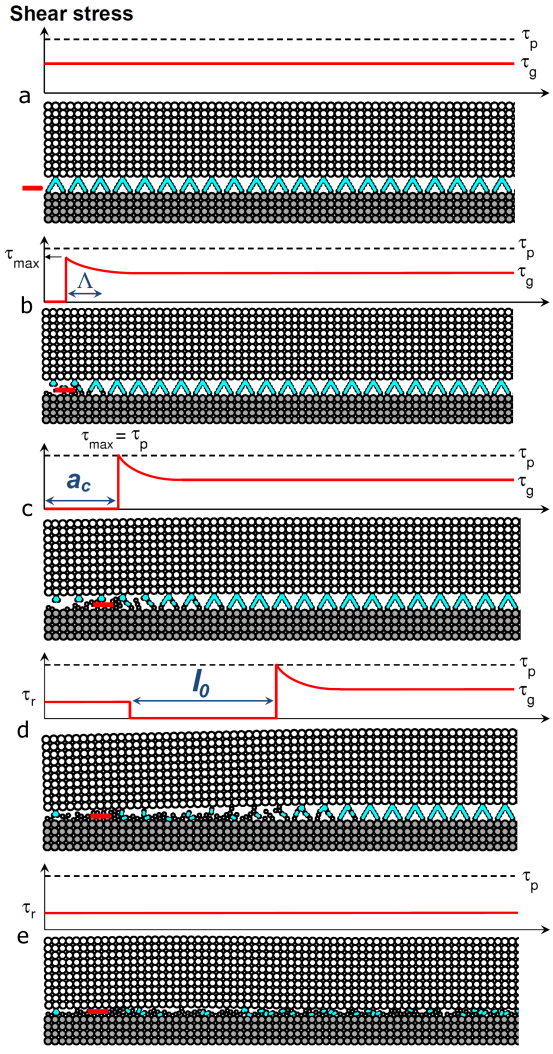

Figure 2: Successive snapshots of a DEM simulation of the propagation saw test (PST). The plots on top of each snapshot represent the shear stress τ (red line) in the WL. τ_p is the WL shear strength (dashed line), $\tau_g = \rho g D \sin\psi$ is the shear stress due to the slab weight and τ_r is the residual frictional stress. The red segment represents the saw used to cut inside the weak layer.

scopic (bulk) properties. For the slab, numerical biaxial tests have been performed to characterize the macroscopic Young's modulus E. For the WL, mixed-mode shear-compression loading simulations were performed to determine the failure envelope (Fig. 3). Through the triangular shape of the WL

The Cryosphere Discuss., doi:10.5194/tc-2016-64, 2016
Manuscript under review for journal The Cryosphere
Published: 13 April 2016

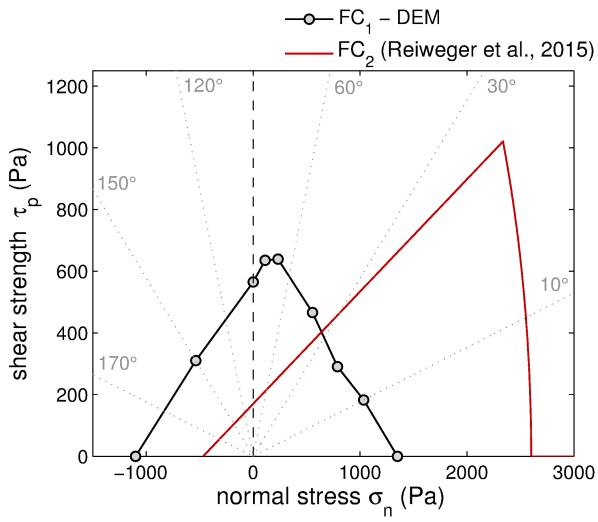

Figure 3: Failure criterion FC_1 of our modeled weak layer (black circles) obtained from mixed-mode shear-compression loading tests. FC_2 is the mixed-mode failure envelope found by Reiweger et al. (2015). The grey dotted lines represent angles of loading ψ such as $\tan\psi = \tau_p/\sigma_n$.

structure, the main features of real WL failure envelopes (Reiweger et al., 2015) are satisfactorily reproduced, with possible failures both in shear and compression (closed envelope).

The applied loading represents a typical PST experiment setup (van Herwijnen and Jamieson, 2005; Gauthier and Jamieson, 2006; Sigrist and Schweizer, 2007). It consists of a combination of gravity (slope angle ψ) and advancing a rigid "saw" (in red in Fig. 2) at a constant velocity $v_{saw} = 2$ m/s through the WL. The saw thickness is $h_{saw} = 2$ mm and the length of the system is $L = 2$ m (Bair et al., 2014; Gaume et al., 2015).

Comparison with propagation saw test (PST) experiments

The dataset consists of 93 PST experiments which were presented in Gaume et al. (2015). It includes the average slab density ρ, slab thickness D, slope angle ψ, WL thickness D_{wl}. The WL specific fracture energy w_f was computed from the penetration resistance using the snow micro-penetrometer (SMP) in the weak layer according to Reuter et al. (2015). The shear strength τ_p of the WL was not measured but we used the mixed-mode shear-compression failure envelope defined by Reiweger et al. (2015) based on laboratory experiments. This failure envelope (in red in Fig. 3), i.e. the relation between the shear strength τ_p and the normal stress σ_n, is described by the following Mohr-Coulomb-Cap model:

$$\tau_p = \tau_p^{mc} = c + \sigma_n \tan\phi \quad \text{for} \quad \psi > \psi_t, \tag{1}$$

The Cryosphere Discuss., doi:10.5194/tc-2016-64, 2016
Manuscript under review for journal The Cryosphere
Published: 13 April 2016

$$\tau_p = \tau_p^{cap} = b\sqrt{1 - \frac{(\sigma_n + \sigma_t)^2}{(\sigma_c + \sigma_t)^2}} \quad \text{for} \quad \psi < \psi_t. \tag{2}$$

with

$$b = K\sqrt{\frac{(\sigma_t + \sigma_c)^2}{(\sigma_t + \sigma_c)^2 - (\frac{K}{\tan\phi})^2}}. \tag{3}$$

The cohesion c (shear strength for $\sigma_n = 0$) can be derived from the WL specific fracture energy using the results of Gaume et al. (2014b):

$$c = \frac{\sqrt{2DE'w_f}}{2l}. \tag{4}$$

$\phi = 20°$ is the friction angle, $\sigma_t = c\tan\phi$ is the tensile strength, $\sigma_c = 2.6$ kPa is the compressive strength and K is the maximum shear strength (Reiweger et al., 2015). The transition between the Mohr-Coulomb and the cap regimes occurs for $\psi = \psi_t = 23°$. Note that, for the 93 PST experiments, the normal stress σ_n was lower than 2 kPa and thus only the Mohr-Coulomb part of the failure envelope (Eq. 1) was used to compute the shear strength τ_p.

The Young's modulus E was derived from density according to Scapozza (2004):

$$E = 5.07 \times 10^9 \left(\frac{\rho}{\rho_{ice}}\right)^{5.19}, \tag{5}$$

with $\rho_{ice} = 917$ kg/m^3. The WL shear modulus G_{wl} was taken constant equal to 0.2 MPa according to the laboratory experiments performed on snow failure by Reiweger et al. (2010) and the Poisson's ratio ν was taken equal to 0.2.

3 Results

DEM simulations

In the simulations, the crack of length a created by the advancing saw in the WL induces tension and bending of the slab, resulting in stress concentrations at the crack tip where the shear stress $\tau = \tau_{max}$ is maximum and larger than the shear stress due to slab weight τ_g. Critical crack length a_c required for the onset of dynamic crack propagation in the WL is reached when τ_{max} meets the shear strength τ_p (Fig. 2c).

We performed a series of systematic simulations to investigate the influence of snow cover parameters on a_c (Fig. 4). Slab properties (slab density ρ, slab elastic modulus E, slab thickness D), WL thickness D_{wl} and slope angle ψ were varied independently in the simulations. Overall, a_c was found to increase with increasing elastic modulus of the slab E and with WL thickness D_{wl}. On the contrary, a_c decreased with increasing slab density ρ, with increasing slab thickness D and with increasing slope angle ψ.

The Cryosphere Discuss., doi:10.5194/tc-2016-64, 2016
Manuscript under review for journal The Cryosphere
Published: 13 April 2016

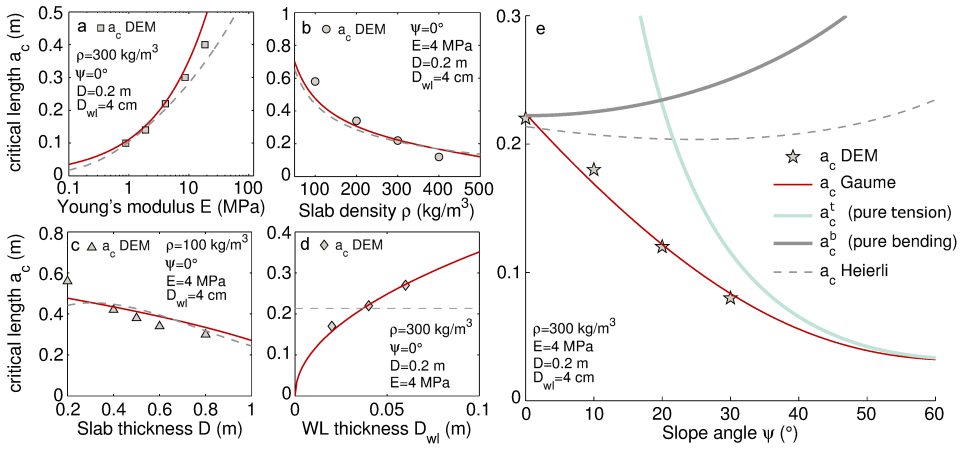

Figure 4: Critical length a_c for crack propagation as a function of (a) the Young's modulus E of the slab, (b) slab density ρ, (c) slab thickness D, (d) WL thickness D_{wl} and (e) slope angle ψ. The symbols represent critical length obtained from the DEM simulations and the solid lines represent the critical length modeled from Eq. 9 and for different failure behaviors. Dashed lines indicate the critical length obtained with the anticrack model (Heierli et al., 2008).

Analytical expression for the critical crack length

The discrete element simulations revealed that the maximum shear stress at the crack tip can be decomposed into two terms related, respectively, to slab tension (τ^t_{max}) and slab bending (τ^b_{max}):

$$\tau_{max} = \tau^t_{max} + \tau^b_{max}. \tag{6}$$

When disregarding slab bending (weak layer with no thickness), the maximum stress τ^t_{max} depends on the shear stress due to the weight of the slab τ_g, the crack length a and a characteristic lengthscale of the system Λ (Chiaia et al., 2008; Gaume et al., 2013, 2014b):

$$\tau^t_{max} = \tau_g \left(1 + \frac{a}{\Lambda}\right) \tag{7}$$

The lengthscale Λ represents the characteristic scale of the exponential decay of the shear stress τ close to the crack tip (Fig. 2b). It is given by $\Lambda = (E' D D_{wl}/G_{wl})^{1/2}$ where $E' = E/(1-\nu^2)$ is the plane stress elastic modulus of the slab and G_{wl} the WL shear modulus (Gaume et al., 2013).

The tension term alone is unable to predict stress concentrations and thus crack propagation on flat terrain ($\psi = 0$), a process that exists, exemplified by numerous field observations (Johnson et al., 2004; van Herwijnen and Jamieson, 2007) and results from our DEM simulations (Fig. 4e). To resolve this discrepancy, the second term in Eq. 6 accounts for slab bending induced by WL collapse. Our DEM simulations showed that this term depends on the normal stress σ_n and the ratio a/Λ

The Cryosphere Discuss., doi:10.5194/tc-2016-64, 2016
Manuscript under review for journal The Cryosphere
Published: 13 April 2016

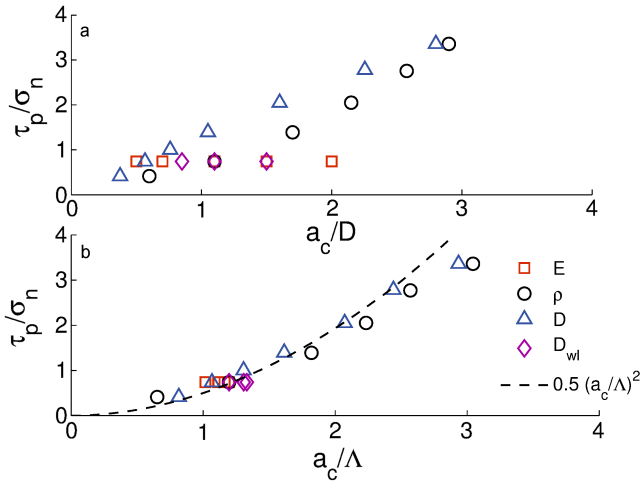

Figure 5: (a) Ratio between the shear strength τ_p and the normal stress σ_n versus the ratio between the critical length a_c and slab thickness D or characteristic length Λ (b) for flat terrain ($\psi = 0°$, i.e. $\tau_g = 0$). The symbol/color in the legend indicates the parameter which was varied in the DEM simulations.

(Fig. 5b) and can be expressed as:

$$\tau^b_{max} = \frac{1}{2}\sigma_n \left(\frac{a}{\Lambda}\right)^2 \tag{8}$$

Note that according to beam theory (Timoshenko and Goodier, 1970), and assuming a rigid WL, $\tau^b_{max} \propto \sigma_n (a/D)^2$, independent of the elastic properties of the slab and the WL. In the present formulation, scaling with a/Λ instead of a/D allows to account for the elastic mismatch between the slab and the WL and to adequately reproduce the numerical results (Fig. 5).

From Eq. 6 the critical length can be obtained by solving $\tau_{max} = \tau_p$ where τ_p is the shear strength given by the failure envelope of the material (Gaume et al., 2015; Reiweger et al., 2015):

$$a_c = \Lambda \left[\frac{-\tau_g + \sqrt{\tau_g^2 + 2\sigma_n\left(\tau_p - \tau_g\right)}}{\sigma_n}\right] \tag{9}$$

Theoretically, this expression is valid only if crack propagation occurs before the slab touches the broken WL, i.e. if the vertical displacement induced by bending remains lower than the collapse height h_c. The length l_0 (Fig. 2d) required for the slab to come into contact with the broken WL can be expressed using beam theory: $l_0 = \left(\frac{2ED^2h_c}{3\rho g \cos\psi}\right)^{1/4}$ (Gaume et al., 2015). For realistic model parameters, a_c was always substantially lower than l_0 ~~(not shown).~~

The agreement between Eq. 9 and results from the DEM simulations is excellent (red solid lines in Fig. 4). We emphasize that scaling of τ^b_{max} with a/Λ is of critical importance. It also provides an

The Cryosphere Discuss., doi:10.5194/tc-2016-64, 2016
Manuscript under review for journal The Cryosphere
Published: 13 April 2016

explanation for the gentler decrease of a_c with D compared to ρ, even though D and ρ equally contribute to the load. Indeed, for a constant load, thicker slabs will result in lower stress concentrations at the crack tip (Eq. 6) due to an increase of Λ.

The predictions of Eq. 9 also compare well with results obtained from 93 PST experiments (Fig. 6). Overall, our model provides very good estimates of the measured critical crack lengths, as demonstrated by the proximity of the data to the 1:1 line. ~~As for the simulations, the critical length in PSTs was always lower than the length~~ l_0 ~~(not shown).~~

4 Discussion

Comparison with the anticrack model

Critical crack lengths predicted by Eq. 9 were compared to the anticrack model (Heierli et al., 2008), for which a_c was computed as function of simulated system parameters (Fig. 4), and by taking a constant specific fracture energy w_f of 0.1 J/m^2. The anticrack model reproduces the influence of E, ρ and D on a_c well for $\psi = 0$, although less accurately than Eq. 9. However, the influence of WL thickness D_{wl} and slope angle ψ on a_c was very poorly reproduced by the anticrack model, both in terms of absolute values and trends. In particular, a slope angle $\psi > 0$ would lead to similar trends of a_c with E, ρ and D but with overestimated values.

The decrease of a_c with slope angle, observed in our DEM results and predicted by Eq. 9, is of particular interest. This trend is in clear contradiction with one of the main outcomes of the anticrack model (Heierli et al., 2008), namely that the critical length is almost independent of slope angle. The discrepancy arises from the fact that the anticrack model (i) assumes that the failure behaviour of the WL is slope independent, (ii) disregards WL elasticity, and (iii) does not correctly account for the interplay between slab tension and slab bending. Concerning WL thickness, a thin WL leads to higher stress concentration in bonds between the grains and thus to a smaller critical crack length (Fig. 4d). This effect cannot be reproduced by the anticrack model due to the rigid character of the WL.

For horizontal terrain, the anticrack model and our new formulation yield similar results. However, this is where the similarities end. Indeed, overall the anticrack model overestimates a_c and more closely resembles a model which accounts for slab bending only: $a_c^b = \Lambda\sqrt{\tau_p/\sigma_n}$ (obtained by solving $\tau_{max}^b = \tau_p$). For steep slopes ($\psi > 30°$), where slab bending becomes negligible compared to tension, critical crack length values obtained from Eq. 9 strongly differ from the prediction of the anticrack model and converge on the contrary towards a purely tensile model: $a_c^t = \Lambda(\tau_p/\tau_g - 1)$ (obtained by solving $\tau_{max}^t = \tau_p$, Fig. 4e).

It should be noted that the anticrack model was validated with only three PST experiments performed at different slope angles (Heierli et al., 2008) and assuming the same snow cover properties. This is somewhat questionable, since snowpack properties can also change with slope angle, thus ob-

The Cryosphere Discuss., doi:10.5194/tc-2016-64, 2016
Manuscript under review for journal The Cryosphere
Published: 13 April 2016

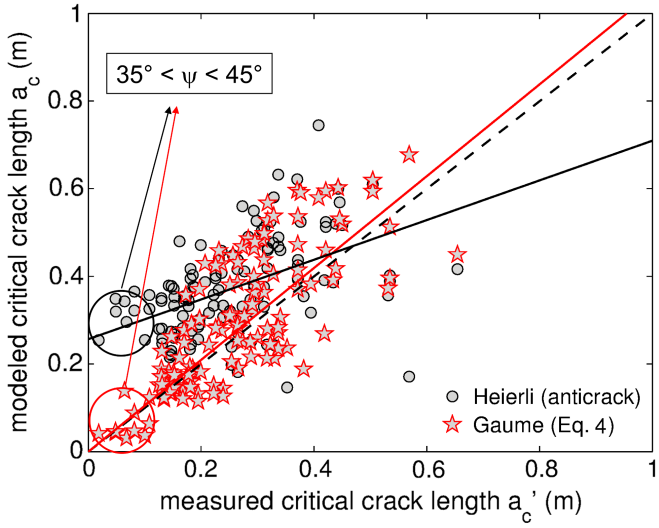

Figure 6: Comparison between measured and modeled critical crack lengths using the anticrack model (Heierli et al., 2008) (black circles) and our new model (Eq. 9, red stars). The continuous lines represents linear fits (in black: $a_c = \gamma_H a_c' + \delta_H$ with $\gamma_H = 0.45$, $\delta_H = 0.23$ and $R_H^2 = 0.22$; in red: $a_c = \gamma_G a_c'$ with $\gamma_G = 1.05$ and $R_G^2 = 0.53$). The dashed line represents the 1:1 line.

scuring the true slope angle dependency. As an example, for their validation, these authors assumed a constant slab thickness $D = 11$ cm over the different slope angles ψ, while in nature, D would generally decreases with increasing ψ. In addition, it is also known that the weak layer strength (Reiweger et al., 2015), slab density (Endo et al., 1998) and thus the elastic modulus (Scapozza, 2004) are strongly slope-dependent. Hence we argue that the dependence of critical crack length with slope angle obtained from a model with constant value of the other parameters should not be compared to the trend observed in the experiments which is the result of a combination of many varying properties. Instead, one should directly compare the measured critical crack length to the modeled one, taking as input parameters the properties measured at the location where the PST was performed.

By comparing the anticrack model to the 93 PST measurements (Fig. 6), we see that a_c is generally overestimated, especially for short critical crack lengths and steep slopes ($35° < \psi < 45°$). For higher values of a_c and gentler slopes, the anticrack predictions better fit with our formulation, even though they still remain mostly above the 1:1 line.

The Cryosphere Discuss., doi:10.5194/tc-2016-64, 2016
Manuscript under review for journal The Cryosphere
Published: 13 April 2016

Relevance and limitations

Performing DEM simulations allowed us to investigate crack propagation in weak snow layers without relying on the same strong assumptions concerning the weak layer as previous research (McClung, 1979; Chiaia et al., 2008; Heierli et al., 2008; Gaume et al., 2014b). For the sake of developing theoretical models, these studies considered either a purely interfacial weak layer (McClung, 1979; Chiaia et al., 2008; Gaume et al., 2014b) or a weak layer composed of a completely rigid material with a slope-independent failure criterion (Heierli et al., 2008). On the contrary, in our simulations, the weak layer is characterized by a finite thickness, an elasticity and a mixed-mode failure envelope in line with recent laboratory experiments (Reiweger et al., 2015). These DEM simulations can thus be seen as numerical laboratory experiments in which the effect of slab and weak layer properties on crack propagation can be investigated independently (which is impossible to do in the field) and from which analytical expressions can be inferred. This important step forward allows to reconcile shear- and collapse-based approaches. For example, our model can describe crack propagation in flat terrain providing the same results as the anticrack model. Furthermore, it predicts the decrease of critical crack length with increasing slope angle in line with shear-based models (McClung, 1979; Chiaia et al., 2008; Gaume et al., 2014b) and in contrast with the anticrack model since the latter assumes rigidity and slope-independent failure of the weak layer.

In a recent study (Gaume et al., 2015), the DEM model was also shown capable of reproducing the dynamic phase of crack propagation as well as fracture arrest in the slab. In particular, the crack propagation speeds and distances obtained from PTV analysis of the PST were well reproduced. Hence, with the present study, we show that our model is able to address the whole crack propagation process.

The main limitation of our model is the uniform character of the slab. In this paper, the multilayered character of the slab was not accounted for, for clarity reasons since the phenomenon is already very complex. However, the elastic modulus of the slab layers has a very important influence on slab deformation and thus on critical crack length (Reuter et al., 2015). For the comparison with the experiments, the elastic modulus was computed from the average slab density. However, in practice, a slab with a homogeneous density ρ will deform differently than a slab of average density ρ with a strong layering contrast. This is probably the reason why significant scattering is observed in Fig. 6 although the overall agreement is good.

Concerning the weak layer, the schematic microstructure considered in this study is sufficient to obtain a realistic failure envelope (Reiweger et al., 2015). Considering more complex microstructures for the weak layer might lead to different behaviors (Gaume et al., 2014a). Nevertheless, Eq. 9 would remain identical, but with possibly different values of shear strength τ_p.

Another important aspect is the relevance of our new model with regards to slab avalanche release. We showed that our model was able to reproduce crack propagation at the scale of the PST. However, at the slope scale, 3D effects, slope-transverse propagation, terrain and snowpack variability ~~might~~

The Cryosphere Discuss., doi:10.5194/tc-2016-64, 2016
Manuscript under review for journal The Cryosphere
Published: 13 April 2016

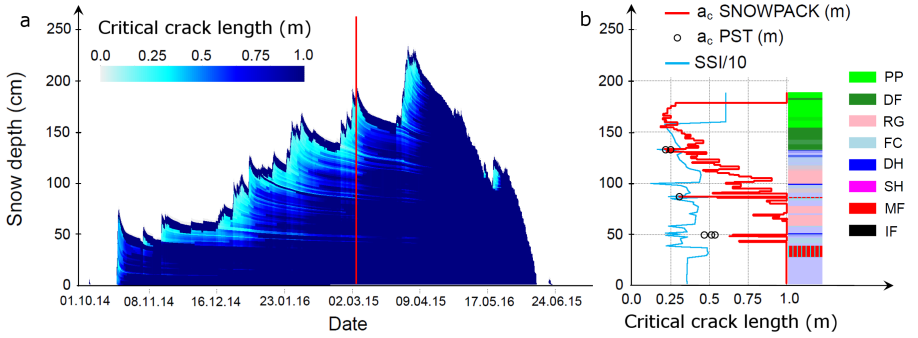

Figure 7: (a) Seasonal profile of the simulated critical crack length (winter 2014-2015) at Steintälli (Davos, Switzerland) on the flat. (b) Vertical profile of critical crack length (modeled and from field PSTs) and SSI/10 for the date marked by the vertical red line in (a). The grain type is shown on the right following Fierz et al. (2009).

make the process even more complex. Nevertheless, it was shown that critical crack length correlates very well with signs of instability (Reuter et al., 2015). In particular, these authors showed that no signs of instability were recorded for $a_c > 0.4$ m while whumpfs, cracks and avalanches were observed for $a_c < 0.4$ m. Hence, our new model of critical crack length can be of major importance in view of avalanche forecasting.

Application to simulated snow stratigraphy

The snow cover model SNOWPACK (Lehning et al., 1999, 2002a, b), which simulates the temporal evolution of snow stratigraphy, is used for operational avalanche forecasting in Switzerland. Potential weak layers in the simulated snow profiles are identified by calculating the structural stability index (SSI), an index based on the balance between shear stress and shear strength (Schweizer et al., 2006; Monti et al., 2012). The SNOWPACK model also provides all necessary variables to determine critical crack length based on Eq. 9. To demonstrate the practical applicability, we performed a simulation for the 2014-2015 winter at the location of an automatic weather station above Davos, Switzerland (Fig. 7). Note that the critical length was arbitrarily set to 1 m in the first 10 cm, since avalanche probability for such shallow layers is generally very low (van Herwijnen and Jamieson, 2007). The same was done when computed values of the critical length exceeded 1 m. Short critical crack lengths clearly highlight potential WLs in the snowpack during the season (Fig. 7a). At the end of the dry-snow season, around 10 April, the percolation of liquid water into the snow cover resulted in a rapid increase in shear strength and thus in larger critical crack lengths throughout the snow cover.

The Cryosphere Discuss., doi:10.5194/tc-2016-64, 2016
Manuscript under review for journal The Cryosphere
Published: 13 April 2016

On 3 March 2015 we performed several PSTs on three WLs at the location of the automatic weather station. The SNOWPACK simulation for that specific day clearly shows local minima in the calculated critical crack length for these three WLs (Fig. 7b). Modeled critical crack lengths were in good agreement with PST field measurements (black circles in Fig. 7b), and SNOWPACK was able to reproduce the observed increase in a_c with increasing depth of the WL. Note that the implementation of Eq. 9 is very sensitive to the parametrization of τ_p used in SNOWPACK (Jamieson and Johnston, 2001; Schweizer et al., 2006). Finally, layers for which critical crack lengths were lower generally also corresponded to layers with local minima in the SSI, suggesting that a combination of SSI and a_c may provide a more reliable instability criterion (Reuter et al., 2015).

5 Conclusions

We proposed a new analytical expression to assess the conditions for the onset of crack propagation in weak snowpack layers. The formulation was developed based on discrete element simulations; it accounts for crucial physical processes involved in crack propagation in snow, namely the complex mechanical behaviour of the WL and the mixed stress states in the slab induced by slab tension and bending resulting from WL collapse. A critical parameter in the formulation is the lengthscale Λ, which accounts for the elastic mismatch between the slab and the WL.

The analytical expression for the critical crack length convincingly reproduced field measurements obtained from 93 propagation saw test experiments. It performed better than the well-known anticrack model which, although correct for flat terrain, significantly overestimated the critical length for steep slopes, where avalanches release. Furthermore, our model predicts that critical crack length decreases with increasing slope angle, in direct contradiction with the anticrack model. This shows that skier-triggered avalanches are more likely on steep rather than on flat slopes, a rather intuitive result. Nevertheless, our model still allows for crack propagation on flat terrain and remote triggering of avalanches, both of which are widely documented by countless field observations.

Finally, our new expression was implemented in the snow cover model SNOWPACK to evaluate critical crack length for all snow layers throughout the entire season. This opens promising perspectives to improve avalanche forecasting by combining traditional stability indices with a new metric to evaluate crack propagation propensity.

Acknowledgements. The critical crack length is implemented in the SNOWPACK model, which is available under the GNU Lesser General Public Licence Version 3 and can be retrieved at http://models.slf.ch. We thank Benjamin Reuter and Bettina Richter for assistance with field data collection. J. Gaume was supported by a Swiss Government Excellence Scholarship and is grateful to the State Secretariat for Education, Research and Innovation SERI of the Swiss Government.

The Cryosphere Discuss., doi:10.5194/tc-2016-64, 2016
Manuscript under review for journal The Cryosphere
Published: 13 April 2016

References

Anderson, T.L.: Fracture Mechanics: Fundamentals and Applications. CRC Press, 640 pp, 2005.

Bair, E., Simenhois, R., van Herwijnen, A., and Birkeland, K.: The influence of edge effects on crack propagation in snow stability tests, The Cryosphere, 8, 1407–1418, 2014.

Brun, E., David, P., Sudul, M., and Brunot, G.: A numerical model to simulate snow-cover stratigraphy for operational avalanche forecasting, J. Glaciol., 38, 13 – 22, 1992.

Chiaia, B., Cornetti, P., and Frigo, B.: Triggering of dry snow slab avalanches: stress versus fracture mechanical approach, Cold Reg. Sci. Technol., 53, 170–178, 2008.

Cundall, P. A. and Strack, O. D. L.: A discrete numerical model for granular assemblies, Géotechnique, 29, 47–65, 1979.

Endo, Y., Kominami, Y., and Niwano, S.: Dependence of new-snow density on slope angle, Ann. Glaciol., 26, 14–18, 1998.

Fierz, C., Armstrong, R., Durand, Y., Etchevers, P., Greene, E., McClung, D., Nishimura, K., Satyawali, P., and Sokratov, S.: The International Classiffcation for Seasonal Snow on the Ground, UNESCO-International Hydrological Program. (Technical Documents in Hydrology), 83, 90 pp, 2009.

Fyffe, B. and Zaiser, M.: The effects of snow variability on slab avalanche release, Cold Reg. Sci. Technol., 40, 229–242, 2004.

Gaume, J., Chambon, G., Eckert, N., and Naaim, M.: Influence of weak-layer heterogeneity on snow slab avalanche release: Application to the evaluation of avalanche release depths., J. Glaciol., 59(215), 423–437, 2013.

Gaume, J., Chambon, G., Reiweger, I., van Herwijnen, A., and Schweizer, J.: On the failure criterion of weak-snow layers using the discrete element method, P. Haegeli (Editor), 2014 International Snow Science Workshop, Banff, Alberta, 2014a.

Gaume, J., Schweizer, J., van Herwijnen, A., Chambon, G., Reuter, B., Eckert, N., and Naaim, M.: Evaluation of slope stability with respect to snowpack spatial variability, J. Geophys. Res., 119, 1783–1789, doi:10.1002/2014JF003193, 2014b.

Gaume, J., van Herwijnen, A., Chambon, G., Birkeland, K., and Schweizer, J.: Modeling of crack propagation in weak snowpack layers using the discrete element method, The Cryosphere, 9, 1915–1932, 2015.

Gauthier, D. and Jamieson, B.: Towards a field test for fracture propagation propensity in weak snowpack layers, J. Glaciol., 52, 164–168, 2006.

Hagenmuller, P., Chambon, G., and Naaim, M.: Microstructure-based modeling of snow mechanics: a discrete element approach, The Cryosphere, 9, 1969–1982, 2015.

Heierli, J., Gumbsch, P., and Zaiser, M.: Anticrack nucleation as triggering mechanism for snow slab avalanches, Science, 321, 240–243, 2008.

Hutchinson, J. W. and Suo, Z.: Mixed mode cracking in layered materials, Advances in applied mechanics, 29, 63–191, 1992.

Jamieson, J. and Johnston, C.: Evaluation of the shear frame test for weak snowpack layers, Ann. Glaciol., 32, 59–69, 2001.

Johnson, B., Jamieson, J., and Stewart, R.: Seismic measurements of fracture speed in a weak layer snowpack layer, Cold Reg. Sci. Technol., 40, 41–45, 2004.

LeBaron, A. and Miller, D.: An Energy-Based Microstructural Constitutive Model for Fracture in Snow, P. Haegeli (Editor), 2014 International Snow Science Workshop, Banff, Alberta, Sept. 29 - Oct. 3, 2014, pp. 134–138, 2014.

Lehning, M., Bartelt, P., Brown, B., Russi, T., Stöckli, U., and Zimmerli, M.: SNOWPACK model calculations for avalanche warning based upon a new network of weather and snow stations, Cold Reg. Sci. Technol., 30, 145–157, 1999.

Lehning, M., Bartelt, P., Brown, B., and Fierz, C.: A physical SNOWPACK model for the Swiss Avalanche Warning Services. Part II: Snow Microstructure, Cold Reg. Sci. Technol., 35(3), 147 – 167, 2002a.

Lehning, M., Bartelt, P., Brown, B., and Fierz, C.: A physical SNOWPACK model for the Swiss Avalanche Warning Services. Part III: Meteorological Boundary Conditions, Thin Layer Formation and Evaluation, Cold Reg. Sci. Technol., 35(3), 169 – 184, 2002b.

McClung, D.: Shear fracture precipitated by strain softening as a mechanism of dry slab avalanche release, J. Geophys. Res., 84(B7), 3519–3526, 1979.

Monti, F., Cagnati, A., Valt, M., and Schweizer, J.: A new method for visualizing snow stability profiles, Cold Reg. Sci. Technol., 78, 64–72, doi:10.1016/j.coldregions.2012.02.005, 2012.

Monti, F., Gaume, J., Van Herwijnen, A., and Schweizer, J.: Snow instability evaluation: calculating the skier-induced stress in a multi-layered snowpack, Nat. Hazard Earth Syst. Sci., 16, 775–788, 2016.

Radjai, F., Dubois, F., et al.: Discrete-element modeling of granular materials, Wiley, 2011.

Reiweger, I., Schweizer, J., Ernst, R., and Dual, J.: Load-controlled test apparatus for snow, Cold Reg. Sci. Technol., 62, 119–125, 2010.

Reiweger, I., Gaume, J., and Schweizer, J.: A new mixed-mode failure criterion for weak snowpack layers, Geophys. Res. Lett., 42, 1427–1432, doi:10.1002/2014GL062780., 2015.

Reuter, B., Schweizer, J., and van Herwijnen, A.: A process-based approach to estimate point snow instability, The Cryosphere, 9, 837–847, 2015.

Scapozza, C.: Entwicklung eines dichte- und temperaturabhängigen Stoffgesetzes zur Beschreibung des visko-elastischen Verhaltens von Schnee, Ph.D. thesis, ETH Zürich, 2004.

Schneebeli, M., Pielmeier, C., and Johnson, J. B.: Measuring snow microstructure and hardness using a high resolution penetrometer, Cold Reg. Sci. Technol., 30, 101 – 114, 1999.

Schweizer, J. and Jamieson, B.: Snowpack tests for assessing snow-slope instability, Ann. Glaciol., 51, 187–194, 2010.

Schweizer, J., Jamieson, B., and Schneebeli, M.: Snow avalanche formation, Rev. Geophys., 41(4), 1016, 2003.

Schweizer, J., Bellaire, S., Fierz, C., Lehning, M., and Pielmeier, C.: Evaluating and improving the stability predictions of the snow cover model SNOWPACK, Cold Reg. Sci. Technol., 46, 52–59, 2006.

Schweizer, J., Kronholm, K., Jamieson, J., and Birkeland, K.: Review of spatial variability of snowpack properties and its importance for avalanche formation, Cold Reg. Sci. Technol., 51(2-3), 253–272, 2008.

Schweizer, J., van Herwijnen, A., and Reuter, B.: Measurements of weak layer fracture energy, Cold Reg. Sci. Technol., 69, 139–144, 2011.

Sigrist, C. and Schweizer, J.: Critical energy release rates of weak snowpack layers determined in field experiments, Geophys. Res. Lett., 34, 2007.

The Cryosphere Discuss., doi:10.5194/tc-2016-64, 2016
Manuscript under review for journal The Cryosphere
Published: 13 April 2016

Thumlert, S. and Jamieson, B.: Stress measurements in the snow cover below localized dynamic loads, Cold Reg. Sci. Technol., 106, 28–35, 2014.

Timoshenko, S. and Goodier, J.: Theory of Elasticity, vol. 37, McGraw-Hill, 1970.

van Herwijnen, A. and Birkeland, K.: Measurements of snow slab displacement in Extended Column Tests and comparison with Propagation Saw Tests, Cold Reg. Sci. Technol., 97, 97–103, 2014.

van Herwijnen, A. and Heierli, J.: A field method for measuring slab stiffness and weak layer fracture energy, Proceedings of the International Snow Science Workshop, Lake Tahoe, CA, USA, 2010, pp. 232–237, 2010.

van Herwijnen, A. and Jamieson, B.: High speed photography of fractures in weak snowpack layers, Cold Reg. Sci. Technol., 43(1-2), 71–82, 2005.

van Herwijnen, A. and Jamieson, B.: Snowpack properties associated with fracture initiation and propagation resulting in skier-triggered dry snow slab avalanches, Cold Reg. Sci. Technol., 50, 13–22, 2007.